

Stochastic Dynamics of Growing Young Diagrams and Their Limit Shapes

P. L. Krapivsky¹

¹*Department of Physics, Boston University, Boston, MA 02215, USA*

We investigate a class of Young diagrams growing via the addition of unit cells and satisfying the constraint that the height difference between adjacent columns $\geq r$. In the long time limit, appropriately re-scaled Young diagrams approach a limit shape that we compute for each integer $r \geq 0$. We also determine limit shapes of ‘diffusively’ growing Young diagrams satisfying the same constraint and evolving through the addition and removal of cells that proceed with equal rates.

I. INTRODUCTION

Partitions of integers frequently appear mathematics, especially in combinatorics, number theory and group representations [1–8]. Partitions are also increasingly popular in physics [9–19]. By definition, a partition of a natural number n is its representation as a sum

$$n = m_1 + \dots + m_k, \quad m_1 \geq \dots \geq m_k > 0 \quad (1)$$

The total number of partitions of n is denoted by $p(n)$. For instance, $4 = 4$, $4 = 3 + 1$, $4 = 2 + 2$, $4 = 2 + 1 + 1$ and $4 = 1 + 1 + 1 + 1$ are all possible partitions of 4. Therefore $p(4) = 5$.

The study of partitions goes back to Leonhard Euler [1]. One his result is the beautiful expression of the generating function encoding the sequence $p(n)$ through a neat infinite product

$$\sum_{n \geq 0} p(n) q^n = \prod_{k \geq 1} \frac{1}{1 - q^k} \quad (2)$$

(It is convenient to set $p(0) = 1$.) Using (2) one easily deduces the asymptotic behavior: $\ln p(n) \simeq 2\pi\sqrt{n/6}$ for $n \gg 1$. Hardy and Ramanujan [2] derived a more precise asymptotic formula

$$p(n) \simeq \frac{1}{4\sqrt{3}n} \exp \left[\pi \sqrt{\frac{2n}{3}} \right] \quad (3)$$

Rademacher improved (3) and derived an *exact* formula [3] for $p(n)$. His proof relies on the so-called circle method of Hardy, Littlewood, and Ramanujan together with marvelous properties of the Dedekind eta function which is ultimately related to the Euler’s generating function (2); see [4] for a pedagogical derivation of the exact Hardy-Ramanujan-Rademacher formula.

One can think about partitions geometrically representing them by Young diagrams. This is illustrated in Fig. 1. The total number $\mathbb{Y}_2(n)$ of Young diagrams composed of n elemental squares is $\mathbb{Y}_2(n) = p(n)$. Rather than fixing an area, one can impose other restrictions, e.g., one can consider Young diagrams that fit into an $a \times b$ box. The total number of such diagrams is

$$\mathbb{Y}(a, b) = \prod_{i=1}^a \prod_{j=1}^b \frac{i+j}{i+j-1} \quad (4)$$

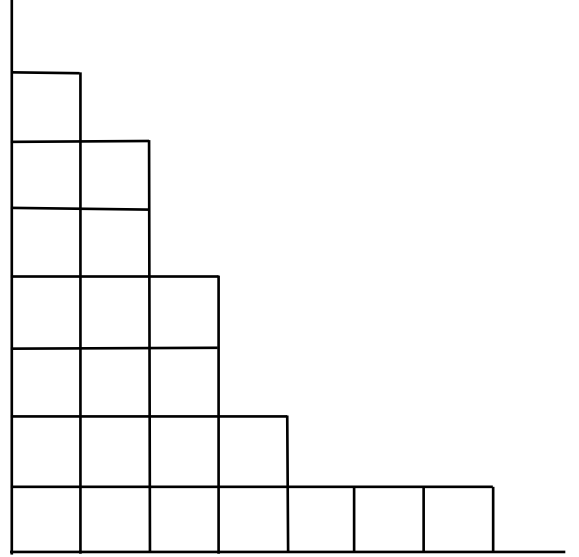


FIG. 1: A Young diagram of a partition of a positive integer n is a diagram with n boxes arranged in columns with non-increasing height. Shown is the Young diagram of the partition $22 = 7 + 6 + 4 + 2 + 1 + 1 + 1$.

The Young diagram is a two-dimensional (lattice) object, and it admits an obvious generalization to higher dimensions. The analog of Eq. (2) is known in three (but not higher) dimensions [5, 7, 20]:

$$\sum_{n \geq 0} \mathbb{Y}_3(n) q^n = \prod_{k \geq 1} \frac{1}{(1 - q^k)^k} \quad (5)$$

where $\mathbb{Y}_3(n)$ is the total number of three-dimensional Young diagrams of ‘volume’ n . This formula was discovered by MacMahon [20] who also found a beautiful formula for the total number $\mathbb{Y}(a, b, c)$ of Young diagrams that fit into an $a \times b \times c$ box generalizing (4):

$$\mathbb{Y}(a, b, c) = \prod_{i=1}^a \prod_{j=1}^b \prod_{k=1}^c \frac{i+j+k-1}{i+j+k-2} \quad (6)$$

Higher-dimensional partitions also appear in physics, e.g., in the context of the infinite-state Potts model [21].

An exact discrete relation follows from Fig. 2, and in the continuum limit it leads to (19). Rescaling the coordinates

$$X = \frac{x}{t}, \quad Y = \frac{y}{t} \quad (20)$$

we re-write (19) as

$$Y = \int_{\max(X-Y, -1)}^1 dZ N(Z) \quad (21)$$

Combining (18) and (21) we obtain an implicit equation for the limit shape

$$4Y = \begin{cases} 1 - 2(X - Y) + (X - Y)^2 & |X - Y| < 1 \\ 0 & X - Y > 1 \end{cases}$$

This equation can be recast into a manifestly symmetric form [37]

$$\sqrt{X} + \sqrt{Y} = 1 \quad (22)$$

in the region $0 < X, Y < 1$.

III. GROWING YOUNG DIAGRAMS WITH UNEQUAL PARTS

Partitions with the requirement that all parts are unequal were already studied by Euler [1] who expressed the generating function for such partitions through an infinite product

$$\sum_{n \geq 0} p_1(n) q^n = \prod_{k \geq 1} (1 + q^k) \quad (23)$$

Here the convention $p_1(0) = 1$ is used again; the index in the partition function $p_1(n)$ reminds about the requirement $m_j - m_{j+1} \geq 1$.

For instance $6 = 6$, $6 = 5 + 1$, $6 = 4 + 2$, $6 = 3 + 2 + 1$ are the only possible partitions of 6 with unequal parts, so $p_1(6) = 4$; the total number of unrestricted partitions of 6 is $p(6) = 11$. Using (23) and analyzing the $q \rightarrow 1$ behavior one can extract the asymptotic behavior: $\ln p_1(n) \simeq \pi \sqrt{n/3}$ as $n \rightarrow \infty$. A more comprehensive analysis [5] gives the Ramanujan asymptotic formula

$$p_1(n) \simeq \frac{1}{4 \cdot 3^{1/4} n^{3/4}} \exp \left[\pi \sqrt{\frac{n}{3}} \right]$$

The limit shape of partitions with unequal parts chosen uniformly among all $p_1(n)$ partitions has been established in Ref. [25] using the generating function (23). In the rescaled coordinates (7) this limit shape reads

$$e^{\lambda X} - e^{-\lambda Y} = 1, \quad \lambda = \frac{\pi}{\sqrt{12}} \quad (24)$$

The limit shape (8) is symmetric with respect to the reflection $X \leftrightarrow Y$, and its span is infinite along both axes.

(From (8) one finds that the span grows logarithmically, $X_* = Y_* = \frac{\sqrt{6}}{2\pi} \ln(n)$, so it diverges in the $n \rightarrow \infty$ limit.) The reflection symmetry is broken for the limit shape (24) and the horizontal span of the partition is finite:

$$X \leq X_* = \frac{\sqrt{12} \ln 2}{\pi} \quad (25)$$

In the original coordinates

$$j \leq j_* = \frac{\ln 2}{\pi} \sqrt{12n}$$

for $n \gg 1$. The maximal horizontal span is $j_{\max} \approx \sqrt{2n}$, it arises for the least tilted partition with strictly decreasing heights: $j_{\max}, j_{\max} - 1, \dots, 1$. Almost all partitions with unequal parts are substantially more narrow:

$$\frac{j_*}{j_{\max}} = \frac{\sqrt{6} \ln 2}{\pi} = 0.54044463946673 \dots$$

We now turn to growing partitions with unequal parts. The first deposition event is the same as before, viz. (10) in the lattice gas framework. The second deposition events is also unique:

$$\bullet \bullet \bullet \bullet \bullet \bullet \circ \circ \circ \circ \circ \circ \implies \bullet \bullet \bullet \bullet \bullet \bullet \bullet \bullet \circ \circ \circ \circ \circ \circ \quad (26)$$

The third deposition event is described by (12), both outcomes occur with the same probability. Analyzing (26), (12), and following deposition events one finds that the underlying lattice gas is a facilitated totally asymmetric simple exclusion process (FTASEP). The crucial difference from the TASEP is facilitation, a particle can hop only when it is pushed from the left (that is, its neighboring left site is occupied).

For the FTASEP we also use the continuity equation (14) on the hydrodynamic level. The FTASEP and closely related models were studied in the past [48–54], and the dependence of the current from the density has been established

$$J(\rho) = \frac{(1 - \rho)(2\rho - 1)}{\rho} \quad (27)$$

To solve the continuity equation (14) with current (27) and the initial condition (16) we employ again the scaling ansatz (17). One gets a rarefaction wave that has been found in Ref. [54]:

$$N(Z) = \begin{cases} 1 & Z < -1 \\ (2 + Z)^{-1/2} & -1 < Z < 1/4 \\ 0 & Z > 1/4 \end{cases} \quad (28)$$

In contrast to shock waves, rarefaction waves usually exhibit a continuous (although not smooth) dependence on coordinate. The rarefaction wave (28) is exceptional, the density jumps from $N = \frac{2}{3}$ at $Z = \frac{1}{4} - 0$ to $N = 0$ at $Z = \frac{1}{4} + 0$ (see Fig. 3).

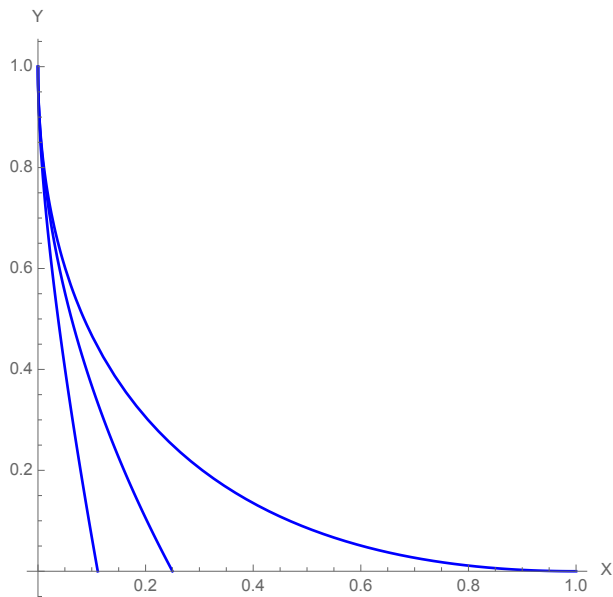


FIG. 4: Top to bottom: The limit shapes with $r = 0, 1, 4$. The limit shape for arbitrary r is given by Eq. (38). In the simplest cases $r = 0$ and $r = 1$, the limit shapes also appear as (22) and (30).

$Z > V(r)$. The non-trivial part of the limit shape is surprisingly simple:

$$Y = 1 - 2\sqrt{X} - (r-1)X, \quad 0 < X < V(r) \quad (38)$$

A few of these non-trivial parts of limit shapes are plotted in Fig. 4. Geometrically, each is a part of a parabola. The area under the parabola (38) is

$$A(r) = \frac{3\sqrt{r} + 1}{6(\sqrt{r} + 1)^3} \quad (39)$$

The area $A(r)$ is a decreasing function of r , see also Fig. 4. In the original coordinates

$$y_{\max} = t, \quad x_{\max} = V(r)t = \frac{t}{(\sqrt{r} + 1)^2} \quad (40)$$

and the area is $A(r)t^2$ in the leading order.

V. DIFFUSIVE GROWTH

In the previous sections, we have studied strictly growing partitions (only deposition events were allowed). We have investigated different types of partitions: arbitrary partitions, partitions with unequal parts, and generally partitions with height difference $\geq r$. In all examples, the growth is ballistic, see (40).

One can allow both additions and removals of squares, requiring that the evolving Young diagram remains the Young diagram of the prescribed type. If the addition

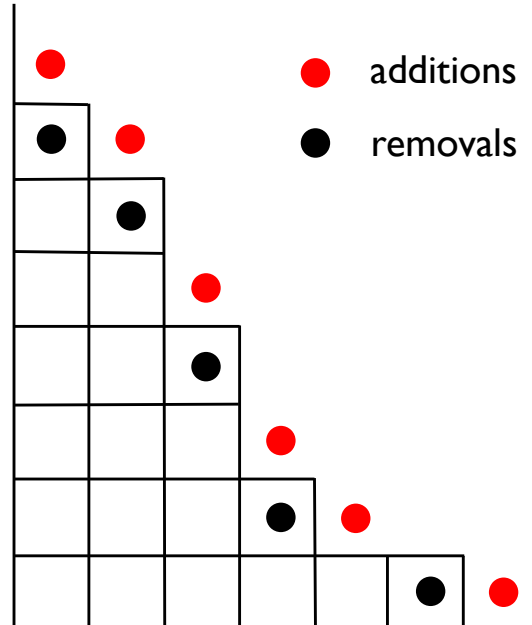


FIG. 5: An illustration of a dynamics acting on the set of arbitrary partitions in which additions and removals of squares occur with the same rates (set equal to unity). Shown is the partition $21 = 7 + 6 + 4 + 2 + 1 + 1$ together with six spots for the addition of squares and five spots for removal. There is always one more spot for addition than for removal, so the average area is $\langle S \rangle = t$ implying that the typical size grows diffusively as \sqrt{t} .

rate exceeds the evaporation rate, the growth remains ballistic, and the limit shapes are the same as before up to a scaling factor. A qualitatively different diffusive growth occurs if additions and removals of squares proceed with equal rates.

Figure 5 illustrates the process with equal rates of additions and removals in the case of arbitrary partitions. The number of positions where new squares can be added always exceeds by one the number of positions from which squares can be removed. Hence the average area increases linearly in time:

$$\langle S \rangle = t \quad (41)$$

In the case of arbitrary partitions the above evolution process maps onto the symmetric simple exclusion process (SSEP) for which the diffusion equation, $\rho_t = \rho_{zz}$, provides the hydrodynamic description. Solving this equation subject to the initial condition (16) one gets

$$\rho(z, t) = \frac{1}{2}\text{Erfc}(\zeta), \quad \zeta = \frac{z}{\sqrt{4t}} \quad (42)$$

which in conjunction with (19) give the limit shape.

A diffusive growth of partitions with unequal parts (Fig. 6) maps onto the facilitated symmetric simple ex-

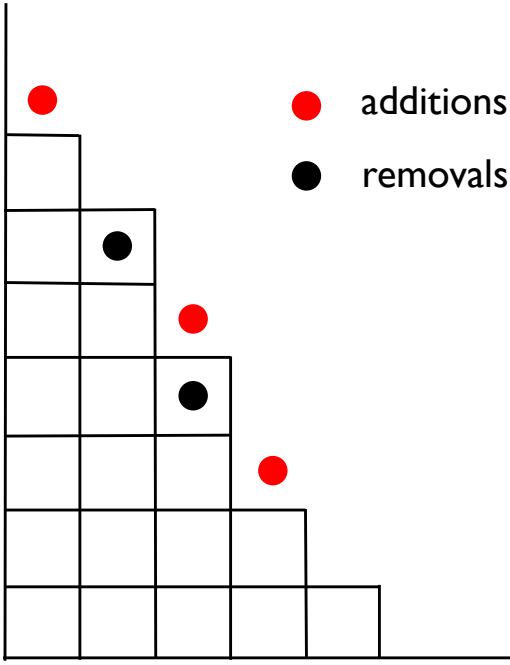


FIG. 6: An illustration of partitions with unequal parts evolving via additions and removals that proceed with equal rates. Shown is the partition of $20 = 7 + 6 + 4 + 2 + 1$ that has three spots for addition and two spots for removal. In this example $m_5 = 1$ and $m_6 = 0$, so the right-most square cannot be removed since $m_5 - m_6 \geq 1$ is required.

clusion process (FSSEP) in which the hopping is facilitated (caused by the nearest neighbor) and symmetric. The hydrodynamic description of the FSSEP is provided by a partial differential equation (PDE)

$$\frac{\partial \rho}{\partial t} = \frac{\partial}{\partial z} \left(\frac{1}{\rho^2} \frac{\partial \rho}{\partial z} \right) \quad (43)$$

This diffusion equation is non-linear since the diffusion coefficient $D(\rho) = \rho^{-2}$ depends on the density. As usual, the hydrodynamic description is applicable when the characteristic spatial and temporal scales greatly exceed the microscopic scales, i.e., the lattice spacing and the inverse hopping rates which we have set to unity. Aside from this generic caveat, for the FSSEP the hydrodynamic description (43) is applicable only when density is sufficiently large, $\frac{1}{2} \leq \rho \leq 1$; in the low-density regime, $0 < \rho < \frac{1}{2}$, the FSSEP quickly reaches a jammed state and the evolution ceases. In a jammed state adjacent particles separated by at least one vacancy.

The expression $D(\rho) = \rho^{-2}$ for the density-dependent diffusion coefficient has been extracted from the diffusion coefficient characterizing a repulsion process [60]. At first sight, these two processes are very different, e.g., the repulsion process has a well-defined hydrodynamic behavior in the entire range $0 \leq \rho \leq 1$. In the $\frac{1}{2} \leq \rho \leq 1$ range, however, both the repulsion process and the FSSEP have

an identical structure of the equilibrium states. Therefore we can use the already known [60] expression of the diffusion coefficient for the repulsion process. The expression $D(\rho) = \rho^{-2}$ for the diffusion coefficient has been also recently derived [61] fully in the realm of the FSSEP.

The solution of Eq. (43) subject to the initial condition (16) has a self-similar form

$$\rho(z, t) = N(\zeta), \quad \zeta = z \sqrt{\frac{\pi}{4t}} \quad (44)$$

By inserting the ansatz (44) into the governing PDE, we reduce Eq. (43) to an ordinary differential equation

$$(N^{-2}N')' + \frac{2\zeta}{\pi} N' = 0 \quad (45)$$

where prime denotes differentiation with respect to ζ . We must solve (45) in the region $-\infty < \zeta < v$.

The boundary condition at $\zeta \rightarrow -\infty$ is

$$N(-\infty) = 1 \quad (46)$$

The density at the right boundary is the minimal allowed density where the hydrodynamic description holds:

$$N(v) = \frac{1}{2} \quad (47a)$$

We need an additional boundary condition since the position of the right boundary, $\zeta = v$, is unknown. The current through it is $-D(\rho)\rho_z = -N^{-2}N'\sqrt{\frac{\pi}{4t}}$. On the other hand, the current is $N\frac{d}{dt}v\sqrt{4t/\pi} = Nv/\sqrt{\pi t}$. Equating these two expressions and using (47a) we get

$$N'(v) = -\frac{v}{4\pi} \quad (47b)$$

The non-linear ordinary differential equation (45) with unknown boundary can be solved analytically. The trick is to map the FSSEP into the SSEP. More precisely, the FSSEP with domain wall initial condition (16) can be mapped into the half-SSEP with a localized source at the boundary as we show in Appendix A. This latter problem is analytically tractable. To determine the density $N(\zeta)$, one must transform both the spatial variable and the density through the spatial variable and the density in the SSEP problem. Completing this program yields the solution in a parametric form

$$N(\zeta) = \frac{1}{1 + \text{Erfc}(\xi)} \quad (48a)$$

$$\zeta = e^{-\xi^2} - \sqrt{\pi} \xi [1 + \text{Erfc}(\xi)] \quad (48b)$$

The derivation of (48a)–(48b) is given in Appendix A.

The density profile (48a)–(48b) describes the density on the half-line $\zeta \leq v = 1$ (see Fig. 7); for $\zeta > 1$, the density vanishes: $N = 0$. (We have included π into the definition of the scaling variable ζ in Eq. (44) to ensure that

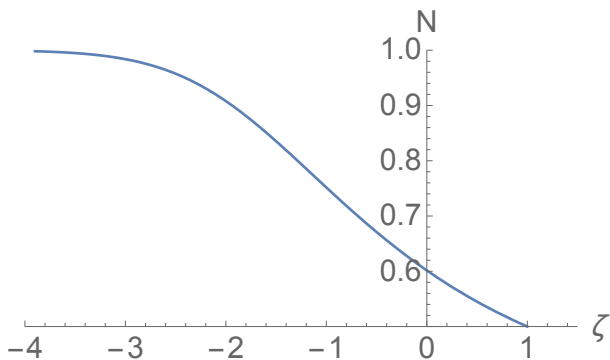


FIG. 7: The scaled density profile (48a)–(48b).

$v = 1$.) Therefore in the original coordinates, the average position of the right-most particle (equivalently, the average width of the diffusively growing partition with unequal parts) is

$$\langle w_t \rangle = \sqrt{\frac{4t}{\pi}} \quad (49)$$

In the re-scaled coordinates

$$X = x\sqrt{\frac{\pi}{4t}}, \quad Y = y\sqrt{\frac{\pi}{4t}} \quad (50)$$

the limit shape is determined via

$$Y = \int_{X-Y}^1 d\zeta N(\zeta) \quad (51)$$

Using Eqs. (48a)–(48b), one computes the integral and recasts (51) into $Y = \sqrt{\pi} \xi(X - Y)$. This is further simplified, with help of Eq. (48b), to a concise equation for the limit shape:

$$e^{-Y^2/\pi} - Y \operatorname{Erfc}(Y/\sqrt{\pi}) = X \quad (52)$$

This limit shape is shown in Fig. 8.

There is one more spot for addition than for removal of squares, so the average area is again given by Eq. (41). This growth law also follows from the diffusion equation (43) thereby providing a consistency check. Indeed, the average area varies with unit rate:

$$\frac{d\langle S \rangle}{dt} = - \int_{-\infty}^{\sqrt{4t/\pi}} dz \rho^{-2} \rho_z = - \int_1^{\frac{1}{2}} \frac{dN}{N^2} = 1 \quad (53)$$

Generally for the diffusive growth of partitions satisfying the requirement $m_j - m_{j+1} \geq r$ the governing PDE is again a non-linear diffusion equation

$$\frac{\partial \rho}{\partial t} = \frac{\partial}{\partial z} \left[\frac{1}{(r\rho - r + 1)^2} \frac{\partial \rho}{\partial z} \right] \quad (54)$$

with density-dependent diffusion coefficient. The hydrodynamic description is applicable in the density range

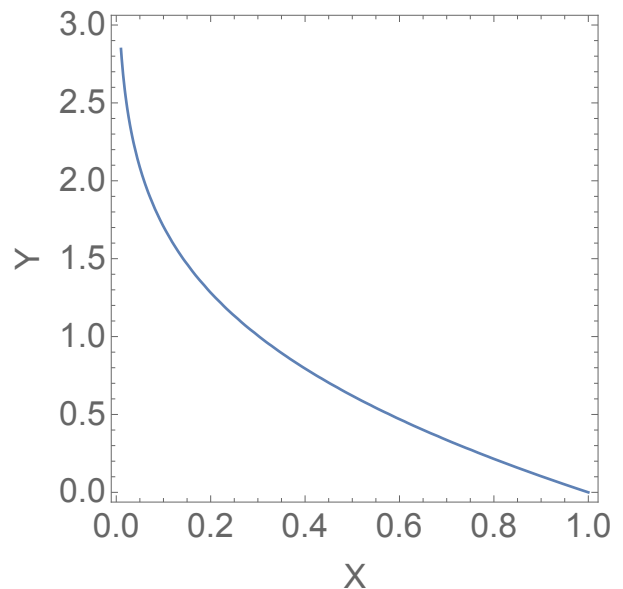


FIG. 8: The limit shape in the case of diffusively growing partitions with unequal parts ($r = 1$). The limit shape is determined by Eq. (52).

$\frac{r}{r+1} \leq \rho \leq 1$, and the diffusion coefficient is again established through the relation to the generalized repulsion process [41, 60]. The solution has a self-similar form (44). The scaling function satisfies

$$[(rN - r + 1)^{-2} N']' + \frac{2\zeta}{\pi} N' = 0 \quad (55)$$

The boundary conditions on the right edge are

$$N(v) = \frac{r}{r+1}, \quad N'(v) = -\frac{2v}{\pi(r+1)^3} \quad (56)$$

Analytical expressions for $v = v(r)$ are unknown for all $r \geq 2$.

VI. CONCLUDING REMARKS

We have computed limit shapes characterizing growing two-dimensional Young diagrams parametrized by a non-negative integer r , the minimal difference between the heights of adjacent columns. Infinitely many limit shapes were also computed [41] for the melting Ising crystals on the square lattice with ferromagnetic spin-spin interactions; these limit shapes are parametrized by the range of interaction.

It would be interesting to study the three-dimensional growing Young diagrams satisfying the constraint that for any (i, j) with $m_{i,j} > 0$, the heights of neighboring columns are smaller at least by r , i.e., $m_{i,j} - m_{i+1,j} \geq r$ and $m_{i,j} - m_{i,j+1} \geq r$. Even for arbitrary Young diagrams, the mapping of the growing interface in three dimensions onto a two-dimensional lattice gas has not

led so far to a scheme allowing to extract a limit shape. One can also try to guess a PDE for the limit shape $z = z(x, y, t)$ satisfying proper symmetry conditions. This approach has led to a prediction [44, 45] tantalizingly close to simulation results. The PDE in the three-dimensional situation admits a generalization to an arbitrary dimension. It would be interesting to guess similar PDEs for restricted classes of Young diagrams.

Acknowledgments. I am grateful to K. Mallick for useful discussions. I also benefitted from the correspondence with G. Barraquand, I. Corwin, and T. Sasamoto.

Appendix A: Diffusively growing partitions with unequal parts

First, we describe the mapping [62] of the FTASEP on the half-TASEP with a source at the boundary. The sites in the TASEP correspond to adjacent particles in the FTASEP. In the TASEP, the site is empty (\square) if adjacent particles are nearest neighbors; if there is a vacancy between adjacent particles, the site is occupied (\blacksquare). Here is an illustration of the evolution (time goes from top to bottom)

$$\begin{array}{ll}
 \dots \bullet \bullet \bullet \bullet \bullet \bullet \circ \circ \circ \dots & \dots \square \square \square \square \\
 \dots \bullet \bullet \bullet \bullet \circ \bullet \circ \circ \dots & \dots \square \square \square \blacksquare \\
 \dots \bullet \bullet \bullet \circ \bullet \bullet \circ \circ \dots & \dots \square \square \blacksquare \square \\
 \dots \bullet \bullet \bullet \circ \bullet \circ \bullet \circ \dots & \dots \square \square \blacksquare \blacksquare \\
 \dots \bullet \bullet \circ \bullet \circ \bullet \circ \bullet \circ \dots & \dots \square \blacksquare \square \blacksquare \\
 \dots \bullet \bullet \circ \bullet \circ \bullet \circ \bullet \circ \dots & \dots \square \blacksquare \square \square
 \end{array} \quad (A1)$$

The lattice model shown on the right is the half-TASEP with particles hopping to the left and new particles entering the right-most site (both processes occur with unit rate). The mapping is one-to-one since starting with initial condition (9) adjacent particles in the FTASEP remain separated by at most one vacancy. The FTASEP process begins with the domain wall initial condition (9) that corresponds to the empty half-line in the half-TASEP, see the top line in (A1).

The mapping of the FSSEP to the half-SSEP with a source at the boundary is identical. In both cases, a simple but crucial observation evident from the example (A1) is that the displacement w_t of the right-most particle for the original process (FTASEP or FSSEP) is the same as the total number of particles in the process obtained by mapping (half-TASEP or half-SSEP).

For the half-SSEP starting with an empty half-line and driven by a source at the boundary, one can solve the exact lattice equations for the density [63, 64], this is even possible for an arbitrary ratio of the input rate to the hopping rate. In long time limit, however, we can set the density at the boundary to unity and deduce the leading behavior from the simpler hydrodynamic framework

$$\nu_t = \nu_{\ell\ell}, \quad \nu(0, t > 0) = 1, \quad \nu(\ell > 0, 0) = 0 \quad (A2)$$

describing the evolution of the density $\nu(\ell, t)$ in the half-SSEP. Solving (A2) one finds

$$\nu(\ell, t) = \text{Erfc}(\xi), \quad \xi = \frac{\ell}{\sqrt{4t}} \quad (A3)$$

Using the identification of the displacement w_t of the right-most particle in the FSSEP with the total number of particles in the half-SSEP, we get

$$\langle w_t \rangle = \int_0^\infty d\ell \nu(\ell, t) = \sqrt{\frac{4t}{\pi}}$$

as was stated in (49).

The mapping between the FSSEP and the half-SSEP tells us that the distance ℓ from the boundary in the half-SSEP corresponds to the distance

$$L = \int_0^\ell du [1 + \nu(u, t)] \quad (A4)$$

from the right-most particle in the FSSEP. Computing the integral in (A4) yields

$$L\sqrt{\frac{\pi}{4t}} = 1 - e^{-\xi^2} + \xi[1 + \text{Erfc}(\xi)] \quad (A5)$$

The spatial coordinate in the FSSEP is $z = \langle w_t \rangle - L$, so the re-scaled spatial coordinate is $\zeta = 1 - L\sqrt{\frac{\pi}{4t}}$. This together with (A5) give Eq. (48b) relating ζ and ξ .

The mapping of the FSSEP into the half-SSEP implies the relation $\rho = 1/(1 + \nu)$ between the corresponding densities. This relation together with (A3) yield the parametric representation (48a) of the density.

Appendix B: Fluctuations

Understanding of fluctuations of growing interfaces, particularly one-dimensional interfaces, has greatly improved over the last 30 years [65–68]. Growing arbitrary partitions have played a crucial role as the first example where fluctuations have been understood [69]. Using the mapping onto the TASEP one can explore fluctuations in the latter framework. For the TASEP starting with the initial condition (9), the quantity that has been particularly well explored is the total number of particles P_t entering the initially empty half-line during time interval $(0, t)$. It was shown [69] that

$$P_t = \frac{t}{4} + t^{1/3} \mathcal{F}_{GUE} \quad (B1)$$

where \mathcal{F}_{GUE} is the Tracy-Widom GUE distribution; the GUE abbreviation reflects that it arises in the Gaussian unitary ensemble of random matrices. (The interface intersects the diagonal at the point (P_t, P_t) , so the fluctuations of the random quantity P_t are directly related to fluctuations of the interface in the $(1, 1)$ direction.)

In the case of growing partitions with unequal parts, and generally, for models with $r > 0$, random quantities like the width of the partition already exhibit intriguing and usually unknown behaviors. First, we show that when $r = 0$, fluctuations of the width and height are Gaussian. This is evident in the lattice gas representation. For instance, the width is the displacement of the right-most particle which is independent of other particles, it merely hops to the right with unit rate. Therefore the width w_t has the Poisson distribution

$$\text{Prob}(w_t = m) = \frac{t^m}{m!} e^{-t} \quad (\text{B2})$$

which is asymptotically Gaussian with fluctuation on the scale $t^{1/2}$. Similarly, the height is the displacement of the left-most vacancy, so it has the same Poisson distribution.

Consider now strictly growing partitions with unequal parts, $r = 1$. In this case, fluctuations of the width w_t have been explored via the mapping into the half-TASEP described in Appendix A. Since the random quantity w_t is equal to the (growing) total number of particles in the half-TASEP, one sees the analogy with the quantity P_t for the TASEP, and hence one expects that fluctuations scale as $t^{1/3}$. This is true, but they follow [62] the GSE Tracy-Widom distribution related to the Gaussian symplectic ensemble of random matrices:

$$w_t = \frac{t}{4} + C_1 t^{1/3} \mathcal{F}_{GSE} \quad (\text{B3})$$

The same \mathcal{F}_{GSE} appears in other growth processes in half-line [70–72], while the \mathcal{F}_{GUE} distribution describes fluctuations of the leading particle in a process studied in Ref. [73]. The behavior of the random quantity w_t for models with $r \geq 2$ is unknown. If the qualitative behavior as in the $r = 1$ case and only the magnitude of fluctuations is affected,

$$w_t = \frac{t}{(\sqrt{r} + 1)^2} + C_r t^{1/3} \mathcal{F}_{GSE} \quad (\text{B4})$$

Finally, let us discuss fluctuations for diffusively growing partitions. In the case of unrestricted partitions, the mapping into the SSEP provides a significant simplification. Fluctuations of the width and height are easy to

understand. The average displacement of the right-most particle can be estimated from the criterion

$$\int_{\langle w_t \rangle}^{\infty} dz \rho(z, t) \sim 1 \quad (\text{B5})$$

Combining (42) and (B5) one gets $\langle w_t \rangle \simeq \sqrt{2t \ln t}$. One can heuristically estimate the variance of the width, $\langle w_t^2 \rangle - \langle w_t \rangle^2$, by arguing that it scales as the square of the average gap $\langle g_t \rangle$ between the right-most particle and the preceding particle. This gap can be estimated from the criterion $\int_{\langle w_t \rangle - \langle g_t \rangle}^{\langle w_t \rangle} dz \rho(z, t) \sim 1$ to give

$$\langle w_t^2 \rangle - \langle w_t \rangle^2 \sim \frac{t}{\ln t} \quad (\text{B6})$$

More precise results are available in the situation when particles undergo Brownian motions [74], while the relevant case of the SSEP is studied in [75].

In the case of partitions with unequal parts, we use again the mapping into the half-SSEP with a source. In addition to the average position of the width, Eq. (49), the variance has been determined [63, 64]. It also exhibits a diffusive growth. The ratio of the variance to the average, the Fano factor, is asymptotically

$$\frac{\langle w_t^2 \rangle - \langle w_t \rangle^2}{\langle w_t \rangle} = 3 - \sqrt{8} \quad (\text{B7})$$

Thus $w_t = 2\sqrt{t/\pi} + t^{1/4}\mathcal{W}$ with a certain (apparently unknown) random distribution \mathcal{W} .

The area is a basic characteristic of the Young diagram supplementing height and width. For unrestricted diffusively growing partitions, fluctuations of the area have been probed in [43]. These fluctuations are strongly non-Gaussian as manifested by the growth of the cumulants: $\langle S^p \rangle_c = A_p t^{(p+1)/2}$. For $p \leq 4$, the amplitudes A_p have been determined analytically [43] using the perturbative approach [76]. For diffusively growing partitions with unequal parts, the computation of the cumulants of the area beyond $\langle S \rangle = t$ seems challenging. The perturbative approach [76] is efficient only for the lattice gases with a constant diffusion coefficient. The mapping on the half-SSEP may help if one would find a simple description of the area in the realm of the half-SSEP.

-
- [1] L. Euler, *Introduction to Analysis of the Infinite* (Springer, New York, 1988).
 [2] G. H. Hardy and S. Ramanujan, Proc. London Math. Soc. **17**, 75 (1918).
 [3] H. Rademacher, Proc. London Math. Soc. **43**, 241 (1937); H. Rademacher, Ann. Math. **44**, 416 (1943).
 [4] T. M. Apostol, *Modular Functions and Dirichlet Series in Number Theory* (Springer-Verlag, New York, 1990).
 [5] G. E. Andrews, *The Theory of Partitions* (Cambridge University Press, New York, 1976).
 [6] W. Fulton, *Young Tableaux, with Applications to Representation Theory and Geometry* (Cambridge University Press, New York, 1997).
 [7] I. G. Macdonald, *Symmetric Functions and Hall Polynomials* (Oxford University Press, Oxford, 1999).
 [8] D. Romik, *The Surprising Mathematics of Longest Increasing Subsequences* (Cambridge University Press, New York, 2015).
 [9] H. A. Bethe, Phys. Rev. **50**, 332 (1936).
 [10] N. Bohr and F. Kalckar, Kgl. Danske Vid. Selskab. Math. Phys. Medd. **14**, 1 (1937).
 [11] F. C. Auluck and D. S. Kothari, Proc. Cambridge Phil.

- Soc. **42**, 272, (1946)
- [12] H. N. V. Temperley, Proc. R. Soc. A **199**, 361 (1949).
- [13] F. Y. Wu, G. Rollet, H. Y. Huang, J. M. Maillard, C. K. Hu, and C. N. Chen, Phys. Rev. Lett. **76**, 173 (1996).
- [14] C. Weiss and M. Holthaus, EPL **59**, 486 (2002).
- [15] M. N. Tran, M. V. N. Murthy, and R. K. Bhaduri, Ann. Phys. **311**, 204 (2004).
- [16] A. Kubasiak, J. K. Korbicz, J. Zakrzewski, and M. Lewenstein, EPL **72**, 506 (2005).
- [17] A. Comtet, S. N. Majumdar, and S. Ouvry, J. Phys. A **40**, 11255 (2007).
- [18] N. Destainville and S. Govindarajan, J. Stat. Phys. **158**, 950 (2015).
- [19] A. Okounkov, Bull. Amer. Math. Soc. **53**, 187 (2016).
- [20] P. A. MacMahon, *Combinatory analysis*, Vol. I & II (Cambridge University Press, Cambridge, 1915–16).
- [21] F. Y. Wu, Math. Comput. Modelling **26**, 269 (1997).
- [22] H. N. V. Temperley, Proc. Cambridge Philos. Soc. **48**, 683 (1952).
- [23] A. M. Vershik and S. V. Kerov, Funct. Anal. Appl. **19**, 21 (1985).
- [24] J.-P. Marchand and Ph. A. Martin, J. Stat. Phys. **44**, 491 (1986).
- [25] A. M. Vershik, Funct. Anal. Appl. **30**, 90 (1996); A. M. Vershik, J. Math. Sci. **119**, 165 (2004).
- [26] A. M. Vershik and Yu. V. Yakubovich, Moscow Math. J. **1**, 457 (2001).
- [27] S. Shlosman, J. Math. Phys. **41**, 1364 (2000).
- [28] P. L. Krapivsky, S. Redner, and J. Tailleur, Phys. Rev. E **69**, 026125 (2004).
- [29] A. M. Vershik and S. V. Kerov, Soviet Math. Dokl. **18**, 527 (1977).
- [30] R. Cerf and R. Kenyon, Commun. Math. Phys. **222**, 147 (2001).
- [31] A. Okounkov and N. Reshetikhin, J. Amer. Math. Soc. **16**, 581 (2003).
- [32] H. Cohn, M. Larsen, and J. Propp, New York J. Math. **4**, 137 (1998).
- [33] H. Cohn, R. Kenyon, and J. Propp, J. Amer. Math. Soc. **14**, 297 (2001).
- [34] A. Okounkov and N. Reshetikhin, Commun. Math. Phys. **269**, 571 (2007).
- [35] R. Kenyon and A. Okounkov, Acta Math. **199**, 263 (2007).
- [36] P. Di Francesco and N. Reshetikhin, Commun. Math. Phys. **309**, 87 (2012).
- [37] H. Rost, Theor. Prob. Rel. Fields **58**, 41 (1981).
- [38] T. M. Liggett, *Interacting Particle Systems* (Springer, New York, 1985).
- [39] D. Kandel and E. Domany, J. Stat. Phys. **58**, 685 (1990).
- [40] M. Barma, J. Phys. A **25**, L693 (1992).
- [41] P. L. Krapivsky and J. Olejarz, Phys. Rev. E **87**, 062111 (2013).
- [42] P. L. Krapivsky, S. Redner and E. Ben-Naim, *A Kinetic View of Statistical Physics* (Cambridge: Cambridge University Press, 2010).
- [43] P. L. Krapivsky, K. Mallick, and T. Sadhu, J. Phys. A **48**, 015005 (2015).
- [44] J. Olejarz, P. L. Krapivsky, S. Redner, and K. Mallick, Phys. Rev. Lett. **108**, 016102 (2012).
- [45] J. Olejarz and P. L. Krapivsky, Phys. Rev. E **88**, 022109 (2013).
- [46] P. L. Krapivsky, Phys. Rev. E **85**, 011152 (2012).
- [47] R. A. Blythe and M. R. Evans, J. Phys. A **40**, R333 (2007).
- [48] T. Sasamoto and M. Wadati, J. Phys. A **31**, 6057 (1998).
- [49] K. Klauack and A. Schadschneider, Physica A **271**, 102 (1999).
- [50] T. Antal and G. M. Schütz, Phys. Rev. E **62**, 84 (2000).
- [51] G. Lakatos and T. Chou, J. Phys. A **36**, 2027 (2003).
- [52] L. B. Shaw, R. K. P. Zia, and K. H. Lee, Phys. Rev. E **68**, 021910 (2003).
- [53] U. Basu and P. K. Mohanty, Phys. Rev. E **79**, 041143 (2009).
- [54] A. Gabel, P. L. Krapivsky, and S. Redner, Phys. Rev. Lett. **105**, 210603 (2010).
- [55] F. D. M. Haldane, Phys. Rev. Lett. **67**, 937 (1991).
- [56] Y. S. Wu, Phys. Rev. Lett. **73**, 922 (1994).
- [57] A. Comtet, S. N. Majumdar, S. Ouvry, and S. Sabhapandit, J. Stat. Mech. P10001 (2007).
- [58] A. Comtet, S. N. Majumdar, and S. Sabhapandit, J. Math. Phys. Anal. Geom. **4**, 24 (2008).
- [59] Equation (35) is difficult to extract from [48–54]. The same current appears in the proper density range for repulsion processes: The top line of Eq. (21) from [60], with $m \rightarrow r$ and $\rho \rightarrow 1 - \rho$, turns into (35).
- [60] P. L. Krapivsky, J. Stat. Mech. P06012 (2013).
- [61] O. Blondel, C. Erignoux, M. Sasada, and M. Simon, Ann. Inst. H. Poincaré Probab. Statist. **56**, 667 (2020).
- [62] J. Baik, G. Barraquand, I. Corwin, and T. Suidan, in: *The Abel Symposium: Computation and Combinatorics in Dynamics, Stochastics and Control*, pp. 1–35 (Springer International Publishing, 2018).
- [63] J. E. Santos and G. M. Schütz, Phys. Rev. E **64**, 036107 (2001).
- [64] P. L. Krapivsky, Phys. Rev. E **86**, 041103 (2012).
- [65] T. Halpin-Healy and Y.-C. Zhang, Phys. Rep. **254**, 215 (1995).
- [66] M. Prähofer and H. Spohn, “Current fluctuations for the totally asymmetric exclusion process,” pp. 185–204 in: *In and Out of Equilibrium: Probability with a Physics Flavor*, ed. by V. Sidoravicius (Birkhäuser, Boston, 2006).
- [67] I. Corwin, Random Matrices Theory Appl. **1**, 1130001 (2012).
- [68] T. Halpin-Healy and K. A. Takeuchi, J. Stat. Phys. **160**, 794 (2015).
- [69] K. Johansson, Commun. Math. Phys. **209**, 437 (2000).
- [70] J. Baik and E. M. Rains, Duke Math. J. **109**, 1 (2001) and Duke Math. J. **109**, 205 (2001).
- [71] J. Baik and E. M. Rains, in: *Random matrix models and their applications*, pp. 1–19 (Cambridge: Cambridge University Press, 2001).
- [72] T. Sasamoto and T. Imamura, J. Stat. Phys. **115**, 749 (2004); T. Sasamoto, J. Stat. Mech. P07007 (2007).
- [73] G. Barraquand and I. Corwin, Ann. Appl. Probab. **26**, 2304 (2016).
- [74] S. Sabhapandit, J. Stat. Mech. L05002 (2007).
- [75] T. Imamura, K. Mallick, and T. Sasamoto, Phys. Rev. Lett. **118**, 160601 (2017).
- [76] P. L. Krapivsky and B. Meerson, Phys. Rev. E **86**, 031106 (2012).